Letter

Exposing the threshold structure of loop integrals

Zeno Capatti[*]

Institute for Theoretical Physics, ETH Zürich, Wolfgang-Pauli-Strasse 27, 8093, Zürich, Switzerland

(Received 1 December 2022; revised 3 February 2023; accepted 3 March 2023; published 24 March 2023)

The understanding of the physical laws determining the infrared behavior of amplitudes is a longstanding and topical problem. In this paper, we show that energy conservation alone implies strong constraints on the threshold singularity structure of Feynman diagrams. In particular, we show that it implies a representation of loop integrals in terms of Fourier transforms of nonsimplicial convex cones. We then engineer a triangulation that has a direct diagrammatic interpretation in terms of a straightforward edge-contraction operation. We use it to develop an algorithmic procedure that performs the Fourier integrations in closed form, yielding the novel cross-free family three-dimensional representation of loop integrals. Its singularity structure is entirely and elegantly expressed in terms of the graph-theoretic notions of connectedness and crossing. These results can be used to study the Kinoshita-Lee-Nauenberg cancellation mechanism, numerically evaluate loop integrals and to simplify threshold regularization procedures.

DOI: 10.1103/PhysRevD.107.L051902

I. INTRODUCTION

The study of the threshold singularity structure of Feynman diagrams and scattering amplitudes is an enduring effort that has, throughout the years, lead to incredible developments that have shed light on the infrared physics of quantum scattering phenomena (see [1] for a review and [1–49] for a historical selection of works on the topic).

Three-dimensional representations of Feynman diagrams, obtained via time-ordered perturbation theory (TOPT) (see [50,51] for a review), via flow-oriented perturbation theory (FOPT) [52], or through the loop-tree duality (LTD) formalism [53–59], are notoriously apt to performing a systematic singularity analysis of Feynman integrals. Indeed, the interplay of energy conservation and residue theorem involved in their derivation makes their singularities directly interpretable in terms of cuts [2]. This in turn allows to leverage a host of graph-theoretical knowledge to perform a diagrammatic study of the structure of physical thresholds. Even then, these three-dimensional representations are plagued by spurious divergences, corresponding to cuts that divide the graph in more than two connected components (TOPT) or cuts containing particles that have both positive and negative on-shell energy (LTD). Even improved LTD formalisms [60–69] that remove spurious singularities by relying on algebraic manipulations of the integrand or direct *Ansätze* are either inadequate for wider generalizations or lack first-principle justification.

In this paper, we derive precise constraints on the singularity structure of a Feynman integral, formulated in terms of the graph-theoretic concepts of crossing and connectedness, by explicitly constructing a three-dimensional representation of loop integrals that manifests them. The analysis formalizes and expands on previous interpretations of such concepts [11,62,64,70–79], such as the exclusion of crossed unitarity cuts [70–72] in the computation of iterated discontinuities.

We exploit methods that pertain to a recently growing branch of literature that applies methods of convex geometry, and more precisely the geometry of polytopes [17,52,73–75,77,78,80–91], to problems in high-energy physics. In particular, we relate Feynman diagrams to Fourier transforms of (nonsimplicial) convex cones. We then perform the Fourier integral analytically using an identity with a digrammatic interpretation in terms of a straightforward edge-contraction procedure.

We provide an algorithm based on the recursive application of edge contraction, resulting in the compact and elegant cross-free family (CFF) representation of loop integrals. Singular denominators are identified with collections of connected subgraphs such that any two subgraphs in the family are either contained one in the other, or do not intersect. Such representation can be cast in factorized form and is especially suited for the numerical evaluation of loop integrals. We provide in the

[*]zeno.ca@gmail.com

Mathematica package `cLTD.m`[1] a generic implementation of the algorithm presented in this paper.

We finally describe the factorization properties of the Fourier transform and the ensuing bound on the scaling of the integrand at the intersection of threshold singularities. The CFF representation and the factorization argument de facto provide a classification of the threshold singularity structure of Feynman diagrams in terms of crossing and connectedness, a fundamental step in the long-standing quest for the understanding of the infrared behavior of Feynman diagrams and amplitudes.

II. ENERGY CONSERVATION

Consider a bridgeless digraph $G = (\mathcal{V}, \mathcal{E})$ with an underlying undirected graph G_u given as a tuple of a set of vertices $\mathcal{V}$ and a set of ordered pairs of vertices $\mathcal{E}$. To each edge $e \in \mathcal{E}$ of the graph is associated a weight $x_e \in \mathbb{R}$, collected in a vector $\mathbf{x} = (x_e)_{e\in\mathcal{E}} \in \mathbb{R}^{|\mathcal{E}|}$. The standard scalar product of two weight vectors $\mathbf{x}$ and $\mathbf{y}$ is $\mathbf{x}\cdot\mathbf{y} = \sum_{e\in\mathcal{E}} x_e y_e$. The component-wise multiplication of two vectors $\boldsymbol{\sigma}$ and $\mathbf{x}$ is denoted as $\mathbf{x}\odot\boldsymbol{\sigma} = (\sigma_e x_e)_{e\in\mathcal{E}}$. Given any subset of the edges $\mathcal{E}' \subseteq \mathcal{E}$, its characteristic vector $\mathbf{1}^{\mathcal{E}'}$ has components $\mathbf{1}^{\mathcal{E}'}_e = 1$ if $e \in \mathcal{E}'$ and $\mathbf{1}^{\mathcal{E}'}_e = 0$ otherwise. The positive (negative) boundary of a subset $S \subset \mathcal{V}$ (also called a cut S) is defined as

$$\delta^+(S) = \{e = \{v, v'\} | v \in S, v' \notin S\}, \tag{1}$$

$$\delta^-(S) = \{e = \{v', v\} | v \in S, v' \notin S\}, \tag{2}$$

and $\delta(S) = \delta^+(S) \cup \delta^-(S)$. Consider the space of weight vectors satisfying energy-conservation constraints, $\mathcal{Q}^0_G \subset \mathbb{R}^{|\mathcal{E}|}$. An element $\mathbf{q}^0_G \in \mathcal{Q}^0_G$ satisfies energy conservation at each vertex:

$$\mathbf{q}^0_G \cdot (\mathbf{1}^{\delta^+(v)} - \mathbf{1}^{\delta^-(v)}) = p^0_v, \quad \forall\ v \in \mathcal{V}, \tag{3}$$

for fixed vertex weights $\{p^0_v\}_{v\in\mathcal{V}}$ with $\sum_{v\in\mathcal{V}} p^0_v = 0$. In Feynman diagrams, p^0_v is the external momentum that injects into the vertex v, which may be chosen to be vanishing. Elements of $\mathcal{Q}^0_G$ can be written in terms of elements of a cycle basis $\mathcal{C}$ of the graph as

$$\mathbf{q}^0_G(\{k^0_c\}_{c\in\mathcal{C}}, \{p^0_v\}_{v\in\mathcal{V}}) = \sum_{c\in\mathcal{C}} \mathbf{s}^G_c k^0_c + \mathbf{p}^0_G(\{p^0_v\}_{v\in\mathcal{V}}), \tag{4}$$

with $L = |\mathcal{C}| = |\mathcal{E}| - |\mathcal{V}| + 1$ and

$$\mathbf{p}^0_G = \sum_{v\in\mathcal{V}} \mathbf{r}^G_v p^0_v. \tag{5}$$

$\mathbf{s}^G_c$ is constructed in the following way: first, $(\mathbf{s}^G_c)_e = s^G_{ce} = 0$ if and only if e does not belong to c. Second, $s^G_{ce} = 1$ if e belongs to the cycle c and the cycle c is oriented in G. Finally, $s^{G'}_{ce} = -s^G_{ce}$, if the orientation for the arc e in G is swapped, yielding a graph G'. The cycle vector so constructed is ambiguous up to a sign, which can be chosen arbitrarily. Analogously, we have $r^{G'}_{ve} = -r^G_{ve}$ (for the purposes of this paper, this is all we need to know about $\mathbf{r}^G_v$).

[1] github.com/apelloni/cLTD.

III. FEYNMAN DIAGRAMS AS FOURIER TRANSFORMS OF CONVEX CONES

A bridgeless Feynman diagram $I_{G_u}(\mathbf{E}, \{p^0_v\}_{v\in\mathcal{V}})$, stripped of its spatial loop integrations, reads

$$I_{G_u} = \int \left[\prod_{c\in\mathcal{C}} \frac{\mathrm{d}k^0_c}{2\pi}\right] \frac{\mathcal{N}_G(\mathbf{q}^0_G)}{\prod_{e\in\mathcal{E}}((q^0_e)^2 - E^2_e + i\varepsilon)}, \tag{6}$$

where $q^0_e = (\mathbf{q}^0_G)_e$ is the linear function of the loop momenta given in Eq. (4) for an arbitrarily chosen digraph G with underlying graph G_u, and $\mathcal{N}_G$ is a polynomial numerator. I_{G_u} is parametric in $\mathbf{E}$, which for applications in quantum field theory (QFT) is the vector of on-shell energies assigned to the edges of the graph, $E_e = \sqrt{|\vec{q}_e|^2 + m^2_e}$. We introduce an auxiliary integration $1 = \int \mathrm{d}x_e \delta(x_e - q^0_e)$ for each edge and use the Fourier representation of the Dirac delta function, which yields

$$I_{G_u} = \int \prod_{c\in\mathcal{C}} \frac{\mathrm{d}k^0_c}{2\pi} \int \mathrm{d}\mathbf{x}\mathrm{d}\boldsymbol{\tau} \frac{\mathcal{N}_G(\mathbf{x}) e^{i\boldsymbol{\tau}\cdot(\mathbf{x}-\mathbf{q}^0_G)}}{\prod_{e\in\mathcal{E}} 2\pi(x^2_e - E^2_e + i\varepsilon)}. \tag{7}$$

This step requires one auxiliary variable for each edge (as in the FOPT derivation [52]) and not for each vertex (as in TOPT).

Contour integration over the variables x_e in Eq. (7) is trivial, as they are not subject to energy conservation. Each propagator contributes two residues, associated to the sign of τ_e and corresponding to the poles $x_e = \pm E_e$, assuming the residue at infinity vanishes. In order for this to be true, $\mathcal{N}$ must be a polynomial in which the energy arguments appear with power at most one, similarly to TOPT. Any diagram can itself be algebraically decomposed into diagrams satisfying this numerator property. For such numerators, I_{G_u} is a sum over $2^{|\mathcal{E}|}$ contributions

$$I_{G_u} = \sum_{\boldsymbol{\sigma}\in\{\pm 1\}^{|\mathcal{E}|}} \frac{\mathcal{N}_G(\boldsymbol{\sigma}\odot\mathbf{E})}{\prod_{e\in\mathcal{E}} 2iE_e} \hat{\mathbb{1}}_{\boldsymbol{\sigma}}(\mathbf{E}, \{p^0_v\}_{v\in\mathcal{V}}), \tag{8}$$

having introduced the function $\hat{\mathbb{1}}_{\boldsymbol{\sigma}}(\mathbf{E}, \{p^0_v\}_{v\in\mathcal{V}})$, given by

$$\hat{\mathbb{1}}_{\boldsymbol{\sigma}} = \int \prod_{c\in\mathcal{C}} \frac{\mathrm{d}k^0_c}{2\pi} \int \prod_{e\in\mathcal{E}} \mathrm{d}\tau_e e^{i\tau_e(\sigma_e E_e - q^0_e)} \Theta(-\sigma_e\tau_e). \tag{9}$$

We will show in Eq. (11) that $\hat{\mathbb{1}}_{\boldsymbol{\sigma}}$ denotes the Fourier transform of a cone. We start by changing integration variables from τ_e to $-\sigma_e\tau_e$, giving

$$\hat{\mathbb{1}}_{\boldsymbol{\sigma}} = \int \prod_{c\in\mathcal{C}} \frac{\mathrm{d}k_c^0}{2\pi} \int_{\mathbb{R}_+^{|\mathcal{E}|}} \mathrm{d}\boldsymbol{\tau} e^{-i\boldsymbol{\tau}\cdot(\mathbf{E}-\boldsymbol{\sigma}\odot\mathbf{q}_G^0)}. \quad (10)$$

Plugging Eq. (4) in $\boldsymbol{\tau}\cdot(\boldsymbol{\sigma}\odot\mathbf{q}_G^0)$ we factorize integration on k_c^0, which is then performed by using the Fourier representation of the Dirac delta function, but in reverse,

$$\hat{\mathbb{1}}_{\boldsymbol{\sigma}} = \int_{\mathbb{R}_+^{|\mathcal{E}|}} \mathrm{d}\boldsymbol{\tau} e^{-i\boldsymbol{\tau}\cdot(\mathbf{E}-\boldsymbol{\sigma}\odot\mathbf{p}_G^0)} \prod_{c\in\mathcal{C}} \delta(\boldsymbol{\tau}\cdot(\boldsymbol{\sigma}\odot\mathbf{s}_c^G)). \quad (11)$$

The Dirac delta functions enforce the integration domain to be the intersection of $|\mathcal{C}|$ hyperplanes with the positive orthant $\mathbb{R}_+^{|\mathcal{E}|}$. Observe that, by definition, $\boldsymbol{\sigma}\odot\mathbf{s}_c^G = \mathbf{s}_c^{G'}$, $\boldsymbol{\sigma}\odot\mathbf{p}_G^0 = \mathbf{p}_{G'}^0$, and $\mathcal{N}_{G'}(\mathbf{E}) = \mathcal{N}_G(\boldsymbol{\sigma}\odot\mathbf{E})$, where G' is the graph obtained from G by swapping the orientation of the edge e if $\sigma_e = -1$. We can thus substitute the sum over $\boldsymbol{\sigma}$ with a sum over digraphs. Let us also observe that, if the graph has an oriented cycle c, then we must have $\boldsymbol{\tau}\cdot\mathbf{s}_c^{G'} = \sum_{e\in c}\tau_e = 0$ in virtue of the Dirac deltas of Eq. (11). Since $\tau_e > 0$ for any $e\in\mathcal{E}$, this implies that the integration domain for the Fourier transform is empty. Consequently, the orientations G that contribute with nonvanishing Fourier transform correspond to directed acyclic graphs. In summary, let $\mathrm{dag}(G_u)$ be the set of all acyclic digraphs with the underlying graph G_u, so that

$$I_{G_u} = \sum_{G\in\mathrm{dag}(G_u)} \frac{\mathcal{N}_G(\mathbf{E})}{\prod_{e\in\mathcal{E}} 2iE_e} \hat{\mathbb{1}}_{\mathcal{K}_G}, \quad (12)$$

with

$$\hat{\mathbb{1}}_{\mathcal{K}_G} = \int_{\mathcal{K}_G} \mathrm{d}\boldsymbol{\tau} e^{-i\boldsymbol{\tau}\cdot(\mathbf{E}-\mathbf{p}_G^0)}, \quad (13)$$

where $\hat{\mathbb{1}}_{\mathcal{K}_G}$ is the Fourier transform of the characteristic function $\mathbb{1}_{\mathcal{K}_G}$ of the cone $\mathcal{K}_G$, defined as

$$\mathcal{K}_G = \{\boldsymbol{\tau}\in\mathbb{R}_+^{|\mathcal{E}|} | \boldsymbol{\tau}\cdot\mathbf{s}_c^G = 0,\ \forall\ c\in\mathcal{C}\}. \quad (14)$$

Only acyclic digraphs contribute to the sum. This is analogous to TOPT, expressed as a sum over vertex orderings, or topological orderings in technical jargon. To each topological ordering corresponds a unique acyclic orientation (in general, not injectively). The relevance of acyclic graphs has also been recognized in the context of causal representations [64]. In dual fashion, FOPT [52] is expressed as a sum over strongly connected digraphs.

IV. TRIANGULATIONS AND THE EDGE-CONTRACTION OPERATION

Before engineering a triangulation of the convex cone $\mathcal{K}_G$, let us discuss the case in which G is a multigraph, i.e., it has multiple edges connecting the same two vertices. Let $e_1, \ldots, e_n$ be a set of edges that connect the same two vertices, v and v'. Let G' be the graph in which all such edges have been substituted by a unique edge e. Then

$$\hat{\mathbb{1}}_{\mathcal{K}_G}(\{E_e\}_{e\in\mathcal{E}}) = \hat{\mathbb{1}}_{\mathcal{K}_{G'}}(\{E_e\}_{e\in\mathcal{E}'})|_{E_e=\sum_{j=1}^n E_j}. \quad (15)$$

In plain words, parallel edges are substituted with a unique edge whose energy equals the sum of their energies. This replacement results in a significant simplification of the combinatorial factors involved in the computation of $\hat{\mathbb{1}}_{\mathcal{K}_G}$. Equation (15) mirrors an analogous treatment of multigraphs presented in [64,77,92].

We now present the fundamental relation required to triangulate the cone $\mathcal{K}_G$. Let G be a simple digraph and let us consider a cut $S\subset\mathcal{V}$. Furthermore, let us impose that $\delta(S) = \delta^+(S)$. The existence of such a cut is guaranteed by the acyclic property. Then

$$\hat{\mathbb{1}}_{\mathcal{K}_G} = \frac{1}{i(\mathbf{E}-\mathbf{p}_G^0)\cdot\mathbf{1}^{\delta(S)}} \sum_{a\in\delta(S)} \hat{\mathbb{1}}_{\mathcal{K}_{G_a}}, \quad (16)$$

where $G_a = (\mathcal{V}_a, \mathcal{E}_a)$ is the graph obtained from G by contracting the edge a. Note that $\mathbf{p}_G^0\cdot\mathbf{1}^{\delta(S)} = \sum_{v\in S} p_v^0$ if $\delta^+(S) = \delta(S)$. Comparison with standard formulas [93] establishes that $\mathbf{1}^{\delta(S)}$ is one of the edge vectors of the cone. Equation (16) is readily derived given that

$$\prod_{e\in\delta(S)} \Theta(\tau_e) = \sum_{a\in\delta(S)} \Theta(\tau_a) \prod_{e\in\delta(S)\backslash\{a\}} \Theta(\tau_e-\tau_a), \quad (17)$$

which expresses the triangulation of the positive orthant $\mathbb{R}_+^{|\delta(S)|}$ in $|\delta(S)|$ cones, each corresponding to the region in which the τ_a is the smallest of all times $\{\tau_e\}_{e\in\delta(S)}$.

Substituting Eq. (17) in $\hat{\mathbb{1}}_{\mathcal{K}_G}$ in Eq. (13), we obtain a sum of $|\delta(S)|$ integrals, labeled by an index $a\in\delta(S)$. For each integral, we perform the change of variables $\tau'_e = \tau_e - \tau_a$, $e\in\delta(S)\backslash\{a\}$, which maps the hyperplane $\boldsymbol{\tau}\cdot\mathbf{s}_c^G = 0$ to $\boldsymbol{\tau}\cdot\mathbf{s}_c^{G_a} = 0$ and the cone $\tau_e > \tau_a > 0$, $e\in\delta(S)\backslash\{a\}$ back to the positive orthant $\mathbb{R}_+^{|\delta(S)|}$, factorizing the integration over τ_a of $e^{i\tau_a\mathbf{1}^{\delta(S)}\cdot(\mathbf{E}-\mathbf{p}_G^0)}$ and yielding Eq. (16).

V. APPLICATIONS

A. Singularities, connectedness, and crossing

In this section we develop an algorithm that uses the contraction operation recursively to perform the Fourier integrations in $\hat{\mathbb{1}}_{\mathcal{K}_G}$, a procedure equivalent to finding a special triangulation of $\mathcal{K}_G$. Such a triangulation is different than that yielding the TOPT representation. The specific triangulation we choose makes the relationship between crossing, connectedness and the threshold singularity structure of Feynman diagrams manifest. A large body of recent works [11,62,64,70–75,77–79] refers to this

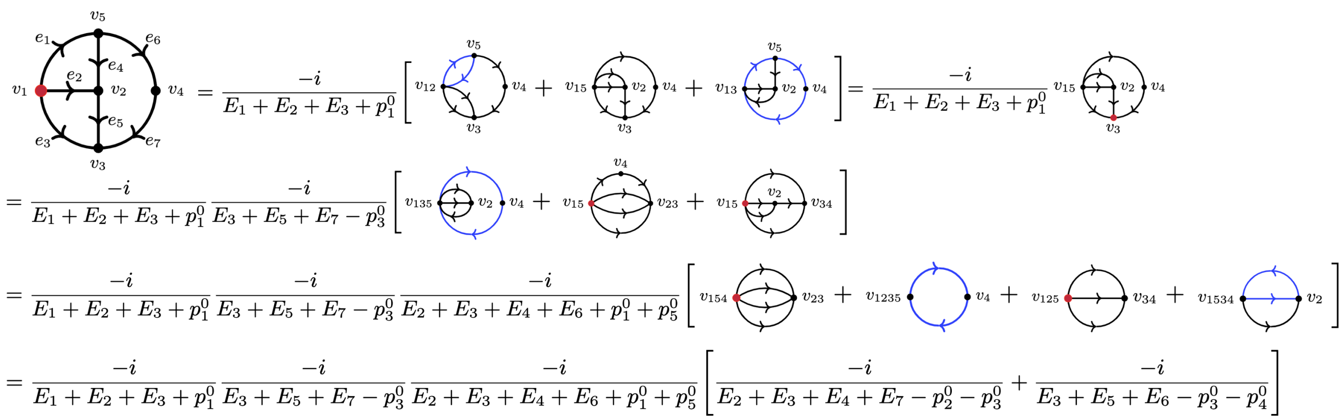

FIG. 1. Graphical depiction of the recursion. The cross-free families generated for this acyclic graph are $\mathcal{F}_G = \{F_1, F_2\}$ with $F_1 = \{\{v_1\},\{v_3\},\{v_1,v_5\},\{v_1,v_5,v_4\}\}$ and $F_2 = \{\{v_1\},\{v_3\},\{v_1,v_5\},\{v_1,v_2,v_5\}\}$. At each iteration of the algorithm, we choose one vertex (highlighted in red) for each of the graphs obtained from the previous iteration, and contract all the edges adjacent to it. All the contracted graphs with directed cycles (highlighted in blue) are excluded.

correspondence with varying degree of rigour and in separate contexts, which motivates looking for an effective and concise description of it. In particular, we will provide a combinatorial and generic construction procedure for the cross-free family representation of Feynman integrals that was conjectured in Eq. (3.44) of [62].

First, given a simple digraph G with vertices labeled as $\mathcal{V} = \{v_{I_1},\ldots,v_{I_n}\}$ for given subsets $I_1,\ldots,I_n \subseteq \mathcal{X}$ of a ground set $\mathcal{X}$ of discrete elements, and given an edge $a = \{v_{I_i}, v_{I_j}\}$ to be contracted, we denote with

$$G_a = (\mathcal{V}\backslash\{v_{I_i}, v_{I_j}\} \cup \{v_{I_i\cup I_j}\}, \mathcal{E}\backslash\{a\}) \tag{18}$$

the contracted graph. This notation maps quantities in the contracted graph to quantities in the original graph. Then given, as an input, the simple, acyclic graph G_i and the family $F_i \subset \mathcal{P}(\mathcal{X})$ [$\mathcal{P}(\mathcal{X})$ being the powerset of $\mathcal{X}$]:

(i) Find a source or a sink v_I of the graph G_i such that $(\mathcal{V}_i\backslash\{v_I\}, \mathcal{E}_i\backslash\delta(v_I))$ is a connected graph. The existence of such vertex is guaranteed by the acyclicity of the digraph G_i. Let $F_{i+1} = F_i \cup \{I\}$.

(ii) Let $\{(G_i)_a\}_{a\in\delta(v_I)}$ be the collection of graphs contracted according to the rule of Eq. (18).

(iii) For each of the graphs $(G_i)_a$, if the graph is not acyclic, terminate and output nothing. If the graph $(G_i)_a$ consists of a single vertex, then terminate and output F_{i+1}. If none of the two applies, then fuse all parallel edges, as described in Eq. (15), so that the resulting graph is also simple and iterate.

This algorithmic procedure is guaranteed to end with a graph consisting of a single vertex. The starting graph G_{init} has vertices $\mathcal{V}_{\text{init}} = \{v_{\{1\}},\ldots,v_{\{n\}}\}$, and $F_{\text{init}} = \emptyset$. It follows that, at each iteration, the set I, as well as any set in F_i, can be mapped to a subset of $\mathcal{V}_{\text{init}}$. The output of the algorithm is a collection of families $\mathcal{F}_G$, dependent on the choice of source or sink at each iteration. Each family $F_{\text{out}} \in \mathcal{F}_G$ is a collection of cuts $S \in F_{\text{out}}$, themselves collections of vertices $S \subset \mathcal{V}_{\text{init}}$. We provide in Fig. 1 an example of the application of the algorithm.

The families of cuts $F_{\text{out}} \in \mathcal{F}$ satisfy that

(i) S and $\mathcal{V}\backslash S$ are connected for any $S \in F_{\text{out}}$.

(ii) F_{out} is a laminar family, that is, for any two sets $S, S' \in F_{\text{out}}$, either S and S' are contained one in the other, or $S \cap S' = \emptyset$.

(iii) F_{out} is obstruction-free, that is, it is not possible to write any set of the family as the union of other sets contained in the family.

We refer to the set F_{out} as a cross-free family. Since at each iteration of the algorithm edge contraction merges two vertices, the cross-free families in $\mathcal{F}_G$ satisfy that $|F_{\text{out}}| = |\mathcal{V}| - 1$. The algorithm effectively performs diagrammatically the triangulation of the cone $\mathcal{K}_G$ in $|\mathcal{F}_G|$ simplicial cones, with each cross-free family $F \in \mathcal{F}_G$ representing a simplicial cone. Using it, one can evaluate $\mathbb{1}_{\mathcal{K}_G}$ for any G and obtain the CFF representation

$$\boxed{I_{G_u} = \sum_{G\in\text{dag}(G_u)} \sum_{F\in\mathcal{F}_G} \frac{i^L(\prod_{e\in\mathcal{E}} 2E_e)^{-1}\mathcal{N}_G(\mathbf{E})}{\prod_{S\in F}(\mathbf{p}_G^0 - \mathbf{E})\cdot \mathbf{1}^{\delta(S)}},} \tag{19}$$

which provides a proof by construction of the representation conjectured in [62]. We provide in the *Mathematica* package `cLTD.m`[1] a generic implementation of this algorithmic procedure, resulting in a ready-to-evaluate integrand.

B. Diagram-level factorization and iterated connectedness

Factorization formulas for Fourier transforms of cones and polytopes can be used to study the leading behavior of the integrand in singular limits [52]. $\hat{\mathbb{1}}_{\mathcal{K}_G}$ itself satisfies a factorization formula. Consider a connected cut S with connected complement and such that $\delta(S) = \delta^+(S)$ and let

$(\mathbf{E}-\mathbf{p}_G^0)\cdot\mathbf{1}^{\delta(S)}=\Delta$. The leading contribution to $\hat{\mathbb{1}}_{\mathcal{K}_G}(\{p_v^0\}_{v\in\mathcal{V}})$ in the expansion in Δ is

$$\hat{\mathbb{1}}_{\mathcal{K}_G}=\frac{\hat{\mathbb{1}}_{\mathcal{K}_{G_1}}(\{p_v^{G_1}\}_{v\in\mathcal{V}_1})\hat{\mathbb{1}}_{\mathcal{K}_{G_2}}(\{p_v^{G_2}\}_{v\in\mathcal{V}_2})}{\Delta}+o(1). \tag{20}$$

$p_v^{G_i}$, $v\in\mathcal{V}_i$, $i=1,2$, are the capacities for the graphs $G_1=(\mathcal{V}_1=S,\mathcal{E}_1)$ and $G_2=(\mathcal{V}_2=\mathcal{V}\backslash S,\mathcal{E}_2)$, obtained from G by deleting the edges in $\delta(S)$. The external energies for the two graphs are defined as follows: if, for a given edge e, we let $v_e^{(1)}$ be its departing vertex and $v_e^{(2)}$ its arriving one, then

$$p_v^{G_i}=\begin{cases}p_v^0+(-1)^i(E_e-p_e^0) & \text{if } v=v_e^{(i)}, e\in\delta(S)\\ p_v^0 & \text{otherwise}\end{cases}. \tag{21}$$

Equation (20) is readily obtained by direct evaluation of the integrals in the variables τ_e, $e\in\delta(S)$ at leading order in Δ. Importantly, if the cut S is disconnected or has disconnected complement, then $\mathbb{1}_{\mathcal{K}_G}=o(1)$.

Given Eq. (20), we now iterate the argument. The singularities of the two graphs G_1 and G_2 correspond to connected cuts such that the complement is also connected. Furthermore, these singularities must correspond to singularities of the original graph G, evaluated at $(\mathbf{E}-\mathbf{p}_G^0)\cdot\mathbf{1}^{\delta(S)}=0$. Thus, let us consider a cross-free family F of cuts (with size $|F|\leq|\mathcal{V}|-1$), and let $(\mathbf{E}-\mathbf{p}_G^0)\cdot\mathbf{1}^{\delta(S)}=\Delta$, for all $S\in F$, and $(\mathbf{E}-\mathbf{p}_G^0)\cdot\mathbf{1}^{\delta(S)}=o(1)$ for $S\notin F$. By iterating the factorization argument, we obtain that a necessary and sufficient condition for

$$\hat{\mathbb{1}}_{\mathcal{K}_G}(\mathbf{E},\{p_v^0\}_{v\in\mathcal{V}})=\frac{w(\mathbf{E},\{p_v^0\}_{v\in\mathcal{V}})}{\Delta^{|F|}}+o(\Delta^{-|F|+1}) \tag{22}$$

to hold with a nonvanishing function w is that the cuts in F divide the graph in $|F|+1$ connected components, which is the lowest possible value. We then say that F satisfies the iterated connectedness property.

The orientation of Fig. 2 results, upon the application of the edge-contraction algorithm, in three cross-free families F_1, F_2, F_3. Consider $F=\{\{v_2\},\{v_5\}\}$, a cross-free subfamily of F_1, F_2, F_3. Thus, in the expansion in $\Delta=(\mathbf{E}-\mathbf{p}_G^0)\cdot\mathbf{1}^{\delta(S)}$, $S\in F$, each term on the right-hand side of the equation in Fig. 2 scales like Δ^{-2}. However, their sum has tamer scaling, Δ^{-1}, since the cuts in F divide the graph in 4 instead of $|F|+1=3$ connected components, in accordance with the bound of Eq. (22).

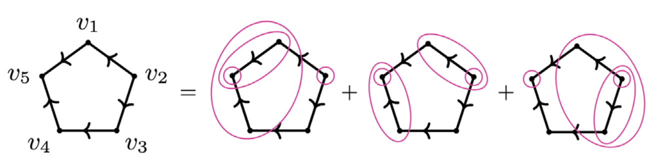

FIG. 2. A diagrammatic way to represent $\mathbb{1}_{\mathcal{K}_G}$ is to draw the cross-free families resulting from the application of the contraction operation, $F_1=\{\{v_5\},\{v_1,v_5\},\{v_1,v_4,v_5\},\{v_2\}\}$, $F_2=\{\{v_5\},\{v_4,v_5\},\{v_1,v_2\},\{v_2\}\}$, $F_3=\{\{v_5\},\{v_2\},\{v_2,v_3\},\{v_1,v_2,v_3\}\}$.

VI. OUTLOOK

In Sec. VA we found a new three-dimensional representation of Feynman diagrams, the cross-free family representation, that is free of spurious singularities and that manifests the relation between thresholds and connected subgraphs as well as the relation between intersections of thresholds and crossing of subgraphs. In Sec. VB, we derived an upper bound on the scaling of three-dimensional representations at the intersection of thresholds. Combined with a simple scaling argument, the bound determines that singularities determined by the intersection of n thresholds of a QCD diagrams are nonintegrable only if the corresponding cuts divide the graph in $n+1$ connected components. This principle may be used to drastically simplify regularization procedures of pinched and nonpinched thresholds [14,94–103].

We conclude by discussing how the analysis of this paper constrains the Kinoshita-Lee-Naunberg (KLN) cancellation [6,7,10–12,62,104–119] of infrared singularities. Consider the quantity P that generalizes the notion of a scattering observable,

$$P=\sum_{n,m=0}^{\infty}a_{nm}P_{nm},\qquad P_{nm}=\mathrm{Tr}\left[\hat{\boldsymbol{\rho}}\hat{\mathbf{S}}_{\mathrm{c}}^n\hat{\mathbf{P}}(\hat{\mathbf{S}}_{\mathrm{c}}^\dagger)^m\right], \tag{23}$$

where $\hat{\boldsymbol{\rho}}$ and $\hat{\mathbf{P}}$ are diagonal sums of on-shell free n-particle states, $|\alpha_1(q_1),\ldots,\alpha_n(q_n)\rangle\langle\alpha_1(q_1),\ldots,\alpha_n(q_n)|$, with weights $f_n^{\hat{\boldsymbol{\rho}}}(\{q_i\}_{i=1}^n)$ and $f_n^{(\hat{\mathbf{P}})}(\{q_i\}_{i=1}^n)$. $\hat{\mathbf{S}}_{\mathrm{c}}$ is the connected S matrix that schematically takes the form

$$\langle\boldsymbol{\alpha}|\,\hat{\mathbf{S}}_{\mathrm{c}}\,|\boldsymbol{\beta}\rangle=\sum_{\substack{\boldsymbol{\alpha}_1\cup\boldsymbol{\alpha}_2=\boldsymbol{\alpha}\\ \boldsymbol{\beta}_1\cup\boldsymbol{\beta}_2=\boldsymbol{\beta}}}\delta_{|\boldsymbol{\alpha}_2||\boldsymbol{\beta}_2|}\quad [\text{diagram}]\,. \tag{24}$$

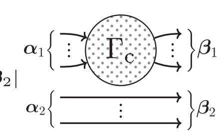

where Γ_{c} is a sum over connected graphs.

Then, P_{nm} is IR-finite provided $f_n^{\hat{\boldsymbol{\rho}}/\hat{\mathbf{P}}}$ satisfy the usual IR-safety constraints. P_{nm} corresponds to sums of interference diagrams that, after deletion of cut edges, necessarily have $n+m$ distinct connected components. This implies that the KLN cancellation mechanism not only holds at the physical observable level (that is, for P), but also for the sum of all interference diagrams that identify a fixed number of connected components. In particular P_{11}, the square sum of connected amplitudes, is IR finite, a staple assumption of all the current methods aimed at the computation of collider observables.

ACKNOWLEDGMENTS

I would like to thank Michael Borinsky, Eric Laenen, and Alex Salas-Bernádez as my collaboration with them inspired me with some of the proof techniques used in this paper. I am also grateful to Valentin Hirschi and Ben Ruijl for countless discussions on the topic, and for their help with the testing of the cross-free family representation as well as with its implementation. I would also like to thank Babis Anastasiou, Hofie Hannesdottir, Dario Kermanschah, and Andrea Pelloni for interesting exchanges on the topic, and Michael Borinsky, Valentin Hirschi, Lucien Huber, and Ben Ruijl for their comments on a draft of this paper. This project has received funding from ETH Zürich under Grant Agreement No. ETH-53 19-2.

---

[1] N. Agarwal, L. Magnea, C. Signorile-Signorile, and A. Tripathi, Phys. Rep. **994**, 1 (2023).
[2] R. E. Cutkosky, J. Math. Phys. (N.Y.) **1**, 429 (1960).
[3] F. Bloch and A. Nordsieck, Phys. Rev. **52**, 54 (1937).
[4] J.-M. Jauch and F. Rohrlich, Helv. Phys. Acta **27**, 613 (1954).
[5] D. Yennie, S. Frautschi, and H. Suura, Ann. Phys. (N.Y.) **13**, 379 (1961).
[6] T. Kinoshita, J. Math. Phys. (N.Y.) **3**, 650 (1962).
[7] T. D. Lee and M. Nauenberg, Phys. Rev. **133**, B1549 (1964).
[8] G. F. Sterman, Phys. Rev. D **17**, 2773 (1978).
[9] G. F. Sterman, Phys. Rev. D **17**, 2789 (1978).
[10] C. Frye, H. Hannesdottir, N. Paul, M. D. Schwartz, and K. Yan, Phys. Rev. D **99**, 056015 (2019).
[11] H. S. Hannesdottir and S. Mizera, *What is the iε for the S-Matrix?* (Springer, New York, 2022).
[12] H. Hannesdottir and M. D. Schwartz, Phys. Rev. D **107**, L021701 (2023).
[13] L. Magnea, J. High Energy Phys. 05 (2021) 282.
[14] Y. Ma, J. High Energy Phys. 05 (2020) 012.
[15] O. Erdoğan and G. Sterman, Phys. Rev. D **91**, 065033 (2015).
[16] R. Akhoury, R. Saotome, and G. Sterman, Phys. Rev. D **84**, 104040 (2011).
[17] T. Binoth and G. Heinrich, Nucl. Phys. **B585**, 741 (2000).
[18] S. B. Libby and G. F. Sterman, Phys. Rev. D **18**, 4737 (1978).
[19] J. Collins, arXiv:2007.04085.
[20] S. Mizera and S. Telen, J. High Energy Phys. 08 (2022) 200.
[21] O. Erdoğan, Phys. Rev. D **89**, 085016 (2014); **90**, 089902 (E) (2014).
[22] C. Heissenberg, Phys. Rev. D **104**, 046016 (2021).
[23] S. Caron-Huot, E. Gardi, J. Reichel, and L. Vernazza, J. High Energy Phys. 03 (2018) 098.
[24] N. Agarwal, A. Danish, L. Magnea, S. Pal, and A. Tripathi, J. High Energy Phys. 05 (2020) 128.
[25] S. Catani and M. H. Seymour, Nucl. Phys. **B485**, 291 (1997); **B510**, 503(E) (1998).
[26] S. Catani, Phys. Lett. B **427**, 161 (1998).
[27] L. J. Dixon, L. Magnea, and G. F. Sterman, J. High Energy Phys. 08 (2008) 022.
[28] T. Becher and M. Neubert, Phys. Rev. Lett. **102**, 162001 (2009); **111**, 199905(E) (2013).
[29] T. Becher and M. Neubert, J. High Energy Phys. 06 (2009) 081; 11 (2013) 24(E).
[30] E. Gardi and L. Magnea, Nuovo Cimento C **32**, 137 (2009).
[31] L. J. Dixon, E. Gardi, and L. Magnea, J. High Energy Phys. 02 (2010) 081.
[32] V. Ahrens, M. Neubert, and L. Vernazza, J. High Energy Phys. 09 (2012) 138.
[33] S. G. Naculich, H. Nastase, and H. J. Schnitzer, J. High Energy Phys. 04 (2013) 114.
[34] T. Becher and M. Neubert, Phys. Rev. D **79**, 125004 (2009); **80**, 109901(E) (2009).
[35] A. Ferroglia, M. Neubert, B. D. Pecjak, and L. L. Yang, J. High Energy Phys. 11 (2009) 062.
[36] E. Gardi, E. Laenen, G. Stavenga, and C. D. White, J. High Energy Phys. 11 (2010) 155.
[37] J. J. Aguilera-Verdugo, F. Driencourt-Mangin, J. Plenter, S. Ramírez-Uribe, G. Rodrigo, G. F. R. Sborlini, W. J. Torres Bobadilla, and S. Tracz, J. High Energy Phys. 12 (2019) 163.
[38] R. Doria, J. Frenkel, and J. C. Taylor, Nucl. Phys. **B168**, 93 (1980).
[39] J. M. Henn and B. Mistlberger, Phys. Rev. Lett. **117**, 171601 (2016),
[40] N. Arkani-Hamed, M. Pate, A.-M. Raclariu, and A. Strominger, J. High Energy Phys. 08 (2021) 062.
[41] Z. Bern, V. Del Duca, W. B. Kilgore, and C. R. Schmidt, Phys. Rev. D **60**, 116001 (1999).
[42] T. Dennen, I. Prlina, M. Spradlin, S. Stanojevic, and A. Volovich, J. High Energy Phys. 06 (2017) 152.
[43] F. Caola, K. Melnikov, D. Napoletano, and L. Tancredi, Phys. Rev. D **103**, 054013 (2021).
[44] G. Parisi, in *Large-Order Behaviour of Perturbation Theory*, Current Physics Sources and Comments Vol. 7, edited by J. Le Guillou and J. Zinn-Justin (Elsevier, New York, 1990), pp. 455–464.
[45] V. Del Duca, Nucl. Phys. **B345**, 369 (1990).
[46] E. Laenen, G. Stavenga, and C. D. White, J. High Energy Phys. 03 (2009) 054.
[47] H. F. Contopanagos and M. B. Einhorn, Phys. Lett. B **277**, 345 (1992).
[48] D. A. Forde and A. Signer, Nucl. Phys. **B684**, 125 (2004).
[49] S. Coleman and R. Norton, Nuovo Cimento Serie **38**, 438 (1965).

[50] G. F. Sterman, *An Introduction to Quantum Field Theory* (Cambridge University Press, Cambridge, England, 1993).
[51] G. F. Sterman, in *Theoretical Advanced Study Institute in Elementary Particle Physics (TASI 95): QCD and Beyond* (1995), pp. 327–408.
[52] M. Borinsky, Z. Capatti, E. Laenen, and A. Salas-Bernárdez, J. High Energy Phys. 01 (2023) 172.
[53] S. Catani, T. Gleisberg, F. Krauss, G. Rodrigo, and J.-C. Winter, J. High Energy Phys. 09 (2008) 065.
[54] I. Bierenbaum, S. Catani, P. Draggiotis, and G. Rodrigo, J. High Energy Phys. 10 (2010) 073.
[55] R. Runkel, Z. Szőr, J. P. Vesga, and S. Weinzierl, Phys. Rev. Lett. **122**, 111603 (2019); **123**, 059902(E) (2019).
[56] R. Runkel, Z. Szőr, J. P. Vesga, and S. Weinzierl, Phys. Rev. D **101**, 116014 (2020).
[57] Z. Capatti, V. Hirschi, D. Kermanschah, and B. Ruijl, Phys. Rev. Lett. **123**, 151602 (2019).
[58] E. T. Tomboulis, J. High Energy Phys. 05 (2017) 148.
[59] M. Berghoff and D. Kreimer, Commun. Number Theory Phys. **17**, 103 (2023).
[60] Z. Capatti, V. Hirschi, D. Kermanschah, A. Pelloni, and B. Ruijl, arXiv:2009.05509.
[61] J. J. Aguilera-Verdugo, F. Driencourt-Mangin, R. J. Hernández-Pinto, J. Plenter, S. Ramirez-Uribe, A. E. Renteria Olivo, G. Rodrigo, G. F. R. Sborlini, W. J. Torres Bobadilla, and S. Tracz, Phys. Rev. Lett. **124**, 211602 (2020).
[62] Z. Capatti, V. Hirschi, A. Pelloni, and B. Ruijl, J. High Energy Phys. 04 (2021) 104.
[63] J. Jesús Aguilera-Verdugo, R. J. Hernández-Pinto, G. Rodrigo, G. F. R. Sborlini, and W. J. Torres Bobadilla, J. High Energy Phys. 02 (2021) 112.
[64] G. F. R. Sborlini, Phys. Rev. D **104**, 036014 (2021).
[65] S. Kromin, N. Schwanemann, and S. Weinzierl, Phys. Rev. D **106**, 076006 (2022).
[66] W. J. T. Bobadilla, Eur. Phys. J. C **81**, 514 (2021).
[67] S. Ramírez-Uribe, R. J. Hernández-Pinto, G. Rodrigo, G. F. R. Sborlini, and W. J. Torres Bobadilla, J. High Energy Phys. 04 (2021) 129.
[68] S. Ramírez-Uribe, R. J. Hernández-Pinto, G. Rodrigo, and G. F. R. Sborlini, Symmetry **14**, 2571 (2022).
[69] W. J. T. Bobadilla, J. High Energy Phys. 04 (2021) 183.
[70] S. Abreu, R. Britto, C. Duhr, and E. Gardi, J. High Energy Phys. 10 (2014) 125.
[71] S. Abreu, R. Britto, C. Duhr, and E. Gardi, J. High Energy Phys. 06 (2017) 114.
[72] J. L. Bourjaily, H. Hannesdottir, A. J. McLeod, M. D. Schwartz, and C. Vergu, J. High Energy Phys. 01 (2021) 205.
[73] P. Benincasa, A. J. McLeod, and C. Vergu, Phys. Rev. D **102**, 125004 (2020).
[74] N. Arkani-Hamed, P. Benincasa, and A. Postnikov, arXiv:1709.02813.
[75] P. Benincasa and W. J. T. Bobadilla, SciPost Phys. **12**, 192 (2022).
[76] F. Pham, Can. Math. Bull. **12**, 534 (1967).
[77] D. Kreimer, Outer space as a combinatorial backbone for Cutkosky rules and coactions, in *Anti-Differentiation and the Calculation of Feynman Amplitudes*, edited by J. Blmlein and C. Schneider (Springer, Cham, 2021).
[78] D. Kreimer and K. Yeats, Adv. Theor. Math. Phys. **27**, 1 (2023).
[79] H. S. Hannesdottir, A. J. McLeod, M. D. Schwartz, and C. Vergu, arXiv:2211.07633.
[80] A. Hodges, J. High Energy Phys. 05 (2013) 135.
[81] N. Arkani-Hamed, J. L. Bourjaily, F. Cachazo, A. B. Goncharov, A. Postnikov, and J. Trnka, *Grassmannian Geometry of Scattering Amplitudes* (Cambridge University Press, Cambridge, England, 2016).
[82] N. Arkani-Hamed and J. Trnka, J. High Energy Phys. 10 (2014) 030.
[83] N. Arkani-Hamed, A. Hodges, and J. Trnka, J. High Energy Phys. 08 (2015) 030.
[84] N. Arkani-Hamed, A. Hillman, and S. Mizera, Phys. Rev. D **105**, 125013 (2022).
[85] M. Borinsky, Ann. Inst. Henri Poincaré D (2020), 10.4171/AIHPD/158.
[86] F. Brown, Commun. Num. Theor. Phys. **11**, 453 (2017).
[87] T. Kaneko and T. Ueda, Comput. Phys. Commun. **181**, 1352 (2010).
[88] A. Pak and A. Smirnov, Eur. Phys. J. C **71**, 1626 (2011).
[89] P. Tourkine, Ann. Henri Poincaré **18**, 2199 (2017).
[90] S. Franco, D. Galloni, A. Mariotti, and J. Trnka, J. High Energy Phys. 03 (2015) 128.
[91] E. Gardi, F. Herzog, S. Jones, Y. Ma, and J. Schlenk, arXiv:2211.14845.
[92] S. Bloch and D. Kreimer, arXiv:1512.01705.
[93] S. Robins, arXiv:2104.06407.
[94] C. Anastasiou and G. Sterman, J. High Energy Phys. 07 (2019) 056.
[95] C. Anastasiou, R. Haindl, G. Sterman, Z. Yang, and M. Zeng, J. High Energy Phys. 04 (2021) 222.
[96] Z. Capatti, V. Hirschi, D. Kermanschah, A. Pelloni, and B. Ruijl, J. High Energy Phys. 04 (2020) 096.
[97] D. Kermanschah, J. High Energy Phys. 01 (2022) 151.
[98] S. Becker, C. Reuschle, and S. Weinzierl, J. High Energy Phys. 12 (2010) 013.
[99] S. Becker, C. Reuschle, and S. Weinzierl, J. High Energy Phys. 07 (2012) 090.
[100] S. Becker and S. Weinzierl, Phys. Rev. D **86**, 074009 (2012).
[101] W. Gong, Z. Nagy, and D. E. Soper, Phys. Rev. D **79**, 033005 (2009).
[102] S. Buchta, G. Chachamis, P. Draggiotis, and G. Rodrigo, Eur. Phys. J. C **77**, 274 (2017).
[103] D. E. Soper, Phys. Rev. D **62**, 014009 (2000).
[104] A. Khalil and W. A. Horowitz, J. Phys. Conf. Ser. **889**, 012002 (2017).
[105] Z. Capatti, V. Hirschi, and B. Ruijl, J. High Energy Phys. 10 (2022) 120.
[106] A. Khalil and W. A. Horowitz, arXiv:1701.00763.
[107] T. Blažek and P. Maták, Eur. Phys. J. C **81**, 1050 (2021).
[108] M. Lavelle and D. McMullan, J. High Energy Phys. 06 (2006) 026.
[109] R. Akhoury, M. G. Sotiropoulos, and V. I. Zakharov, Phys. Rev. D **56**, 377 (1997).
[110] G. F. R. Sborlini, F. Driencourt-Mangin, R. Hernandez-Pinto, and G. Rodrigo, J. High Energy Phys. 08 (2016) 160.
[111] C. Gómez, R. Letschka, and S. Zell, J. High Energy Phys. 09 (2018) 115.

[112] D. Carney, L. Chaurette, D. Neuenfeld, and G. W. Semenoff, Phys. Rev. Lett. **119**, 180502 (2017).

[113] K. Melnikov and V. Serbo, Nucl. Phys. **B483**, 67 (1997).

[114] C. Di'Lieto, S. Gendron, I. Halliday, and C. Sachrajda, Nucl. Phys. **B183**, 223 (1981).

[115] W. Frazer and L. van Hove, Physica (Utrecht) **24**, 137 (1958).

[116] C. Carneiro, M. Day, J. Frenkel, J. Taylor, and M. Thomaz, Nucl. Phys. **B183**, 445 (1981).

[117] T. Kinoshita, Prog. Theor. Phys. **5**, 1045 (1950).

[118] T. Muta and C. A. Nelson, Phys. Rev. D **25**, 2222 (1982).

[119] A. Axelrod and C. A. Nelson, Phys. Rev. D **32**, 2385 (1985).